

DESIGN OF LEAPING BEHAVIOR IN A PLANAR MODEL WITH THREE COMPLIANT AND ROLLING LEGS*

YA-CHENG CHOU, KE-JUNG HUANG, WEI-SHUN YU, AND PEI-CHUN LIN[†]

*National Taiwan University, Mechanical Engineering
No.1 Sec. 4 Roosevelt Rd., ME, Eng. Bldg.
Taipei 106, Taiwan*

We report on the development of a planar three-leg robot model for leaping behavior. The model is composed of a rigid body and three massless legs. The model for each leg is extracted from the virtual leg model of a rolling spring loaded inverted pendulum, which has two segments connected by a torsional spring. The quantitative equations of motions are formulated. By evaluating the dynamic behavior of the three-leg model, a 2-step leaping maneuver is developed. During the 1st-step leaping, the running legs thrust to induce a leap of the body. This leap serves two purposes: to provide sufficient time for the legs to reconfigure their poses; and to adjust the body pitch, preparing for the 2nd-step leap. After the robot lands on the ground with the desired body pose and leg configurations, all legs provide full thrust and initiate the 2nd-step leaping, which makes the body fly over the obstacle. The trajectory for leaping behavior is designed based on this dynamic model and is implemented in the RHex-style robot for experimental evaluation.

1. Introduction

Leaping is one of the unique actions performed by legged animals, which allows them to rapidly change their motion status. Animals use leaping in life-dependent activities such as hunting prey or escaping from predators. Animals also leap to overcome rough terrain and obstacles. For a robot, leaping behavior is also desirable. Land textures are often rough, whether in natural or artificial environments, and leaping can negotiate this rough terrain much faster than other types of gaits such as crawling.

Because inducing leaping/jumping motion on the robot usually requires actuators with considerable power to maneuver the body in a specific manner, it is difficult to generate this behavior on ordinary robots designed for walking or running. Therefore, jumping-specialized robots have been designed, while some walking robots were equipped with extra actuators and mechanisms for jumping. Examples include the miniature 7g jumping robot [1], the robot Grillo [2], the

* This work is supported by the National Science Council (NSC), Taiwan, under contract 100-2628-E-002 -021 -MY3.

[†] Corresponding information: peichunlin@ntu.edu.tw

frog robot Mowgli [3], the Mini-Whegs [4], and the wheeled robot SandFlea [5]. Few works relate to jumping-like behavior in the ordinary walking/running robots. On the simulation side, Wong et. al. simulated a quadruped performing a standing jump over an obstacle [6]. On the robot side, the quadruped LittleDog can jump to pass an obstacle by an optimization method [7]. The Hexapod RHex can jump in small steps by a pronking gait [8]. The robot PAW can jump a short step by matching front and hind leg motions [9]. However, the motions performed by the above empirical robots are not leaping behavior with large-scale ballistic flight. To the best of our knowledge, the quadruped BigDog is the only robot showing leaping behavior which is transient from running. However, the demonstration was revealed only in movie clips with no detailed documentation released [10].

Aiming to develop leaping behavior and its transition from ordinary running behavior in an empirical RHex-style robot, we report on the development of a planar reduced-order model, which serves as a guideline for determining how the legs of the robot should move. The main contribution of this work lies in the methodology of model construction, analysis of the model's behavior, and the systematic variation of the reduced-order parameters to search for a feasible domain of leaping behavior.

2. Model Formulation

Because leaping behavior mainly resides on the robot state in the sagittal plane, a planar model is desired. We also found that the intrinsic model for running (such as a spring-loaded inverted pendulum (SLIP) with only one virtual leg) is not entirely suitable for fast state changes. Thus, a three-leg model was designed, which is composed of a front leg, a middle leg, and a hind leg as shown in Figure 1(a). This model preserves the six-legged structure of insects or hexapod robots by collapsing the right and left legs into one. The body is modeled as a rigid body with mass m at center of mass (COM) and with mass moment of inertia I_b , and the legs are modeled as massless springs. In addition to focusing on the model development, experimental verification is set as the final step of this work. Thus, the dynamic behavior of the experimental platform (i.e., the RHex-style robot [11]) should be considered in the modeling work. The compliant half-circular leg of the RHex-style robot has two characteristics which cannot be captured by an ordinary linear spring—rolling contact and varying compliance which is determined by the contact point at every instant. Thus, instead of the linear virtual spring that is widely utilized in the traditional spring-loaded inverted pendulum (SLIP) model, we adopted a leg model with a rolling contact and torsional spring, as reported in the recently-developed Rolling SLIP (R-SLIP) [12]. The virtual leg in the R-SLIP model has a point mass and two segments connected by a torsional spring. The lower segment has a circular shape, providing rolling contact to the ground. During the rolling motion, because the length of moment arm changes, the equivalent linear stiffness between the robot's hip (or point mass) and ground-contact point varies

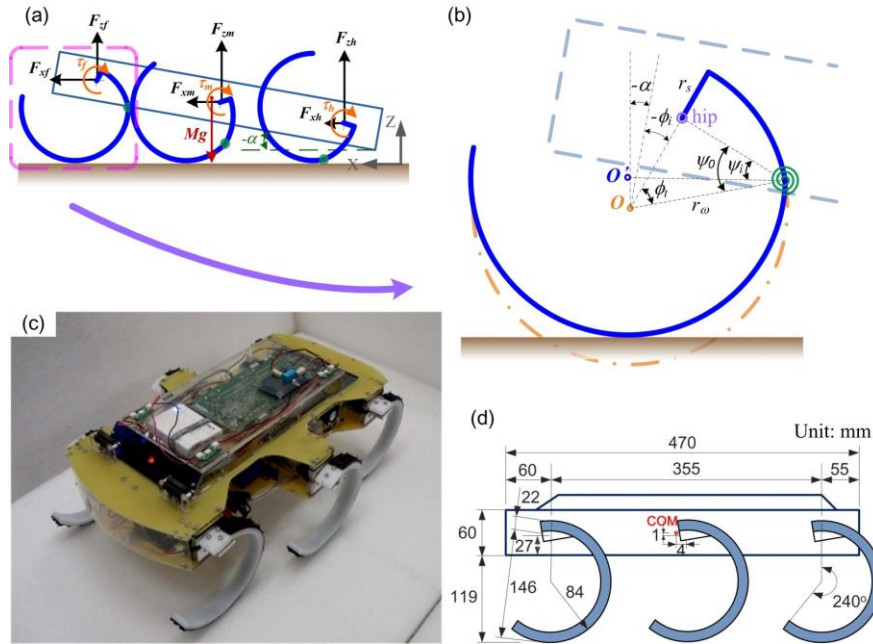


Figure 1. Illustration of the three-leg model (a)(b) and the experimental platform, the RHex-style robot (c)(d): (a) Overall illustration; (b) parameter definitions of the leg portion, where the robot body is sketched in dashed lines. The leg is composed of two segments (blue solid line and arc) connected by torsion springs (green spiral). The leg in its neutral configuration is plotted in an orange dash-dotted arc; (c) photo of the RHex-style robot; (d) dimensions of the robot.

accordingly. Thus, two characteristics of the half-circular leg described above can be adequately captured. Figure 1(b) shows leg parameters defined for model development: O is the center of the circular leg without leg compression; r_o and r_s are leg geometrical parameters; ϕ_i and ψ_o are intrinsic leg parameters which present configuration of the torsion spring in its natural configuration; α is body pitch angle and $\phi_{i=f,m,h}$ is orientation of the leg with respect to the robot body. The subscripts f , m , and h represent front, middle, and hind, respectively. When the leg contacts the ground and the torsion spring is compressed, the center of the circular leg moves to O' and the spring configuration can be captured by ψ_i . The legs are assumed to have pure rolling contact to the ground. With this assumption, the leg rotation angles, $\phi_{i=f,m,h}$, and leg compressions, $\psi_{i=f,m,h}$, are related to each other. As a result, the degrees of freedom (DOFs) of the model is reduced to three, and the three variables used to state the model formulation are orientation of the hind leg, ϕ_h , compression status of the hind leg, ψ_h , and body pitch angle, α .

We now give a brief description of the quantitative model formulation. There are nine external forces/moments acting on the body as shown in Figure 1(a), where each hip has one torque, $\tau_{i=f,m,h}$, and two reaction forces, F_{xi} and F_{zi} , in the horizontal (x) and vertical (z) axes. With these definitions,

two force equations and one moment equation of motion (EOM) can be formulated. The acceleration of the body COM in EOMs can be derived by the configuration relating the hind leg to the COM. The torques in EOMs are motor torques, and these can be computed according to the DC motor model, which sets the motor torque as the function of the supplying voltage V_i ($i=f,m,h$), motor speed (i.e., equal to hip speeds, $\dot{\phi}_i$ ($i=f,m,h$)), and motor internal characteristics. The reaction forces can then be computed according to static equilibrium. Finally, by importing motor torque, hip forces, and body acceleration into the EOMs, the equations of motion in state-space can be represented as:

$$\frac{d}{dt} \begin{bmatrix} \phi_h \\ \dot{\phi}_h \\ \psi_h \\ \dot{\psi}_h \\ \alpha \\ \dot{\alpha} \end{bmatrix} = \begin{bmatrix} \dot{\phi}_h \\ f_1(\phi_h, \dot{\phi}_h, \psi_h, \dot{\psi}_h, \alpha, \dot{\alpha}, V_i) \\ \dot{\psi}_h \\ f_2(\phi_h, \dot{\phi}_h, \psi_h, \dot{\psi}_h, \alpha, \dot{\alpha}, V_i) \\ \dot{\alpha} \\ f_3(\phi_h, \dot{\phi}_h, \psi_h, \dot{\psi}_h, \alpha, \dot{\alpha}, V_i) \end{bmatrix}_{i=f,m,h} \quad (1)$$

With initial conditions and (1), the motion of the model in the stance phase can be simulated numerically until the model takes off for ballistic flight. Note that in the empirical evaluation, because ϕ_h , $\dot{\phi}_h$, and ψ_h are hard to measure and justify, these three states are further represented as a function of the COM displacement and velocity, where the mapping is one-to-one. Thus, the model can be regarded as having five varying initial conditions: α_0 , $\dot{\alpha}_0$, Z_{c0} , \dot{X}_{c0} and \dot{Z}_{c0} as well as one fixed: ψ_h (i.e., simulation starts with the legs in a natural configuration). After the robot takes off, it moves according to the ballistic model.

3. Design of Leg Maneuver for Leaping Behavior

In general, if the legs of the robot (i) have sufficient DOFs for posture maneuver and (ii) have enough instantaneous power for fast leg-state changes, the robot may be able to transition from running to leaping in one step. However, the experimental platform for this work, the RHex-style robot, has only one active rotational DOF per leg. Though various behaviors can already be developed within this simple mechanical structure [11, 13, 14], the maneuverability of the body posture in a fast and dynamic manner is indeed limited. In addition, we also found that the motor power of the present robot is not enough to change phases of the tripods from 180 degrees (i.e., alternating tripod gait) to 0 degrees (i.e., leaping with all legs) in one stride. Therefore, a two-step leaping behavior is required to excite successful leaping in the RHex-style robot. The 1st-step leap serves two purposes: to adjust the body posture (i.e., pitch) and for practical implementation, to synchronize the phases of all legs in

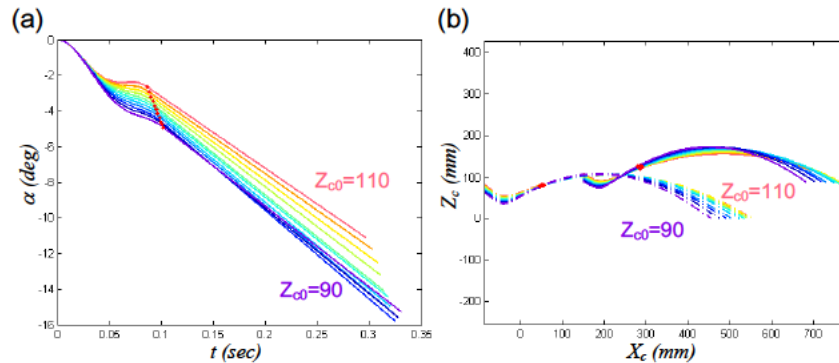


Figure 2. Simulation of various body states versus time with varying initial body height Z_{c0} (unit: mm) in the 1st-step leaping: (a) body pitch and (b) COM trajectory. Red dots represent take-off moment.

two tripods. In consequence, the body can adequately leap with full thrust from all legs in the 2nd-step leap.

Leaping is initiated and transient from tripod running, so the body state in running determines the initial conditions for leaping. Because the variation in pitch during running is small, the horizontal body posture (i.e., α_0 and $\dot{\alpha}_0$ at zero) can be treated as the initial condition for leaping, where the distances between the three hips and the ground are the same. At this configuration, if the three ground-contact legs (i.e., one tripod) are simultaneously driven with full power, the body state is varied as shown in Figure 2, where Z_{c0} is the initial body height. We specifically chose Z_{c0} as the active variable since it is the only variable which can be maneuvered easily in empirical operation among five initial conditions in the model (i.e., α_0 , $\dot{\alpha}_0$, Z_{c0} , \dot{X}_{c0} and \dot{Z}_{c0}). Figure 2(a) clearly reveals an important fact that, no matter at which body height Z_{c0} the robot starts to thrust, the body pitch decreases (i.e., head-up). This phenomenon is undesirable since the back side of the robot may hit the obstacle during leaping, and this posture is also not adequate to transition to running after leaping. Thus, in the current model formulation one-step leaping is not achievable. Because head-up of the model in 1st-step leaping is unavoidable, the 2nd-step leap is investigated with the initial conditions where the body is head-up. Figure 3 plots various states with time when the robot starts to thrust with full power at different initial body pitches, varying from -7° to -12° . Figure 3(a) reveals that the profiles of body pitch versus time can be dramatically different with different initial body pitches. In addition, final body pitch could be dramatically different from its initial head-up condition, which is desirable since this phenomenon allows the body pitch to be adjusted back to the desired level after leaping. As a result, to allow 2nd-step leaping to successfully fly over the obstacle, a suitable initial body pitch can be selected to make the final after-flight pitch more horizontal for proper landing. The figure reveals that -10° is around the right range.

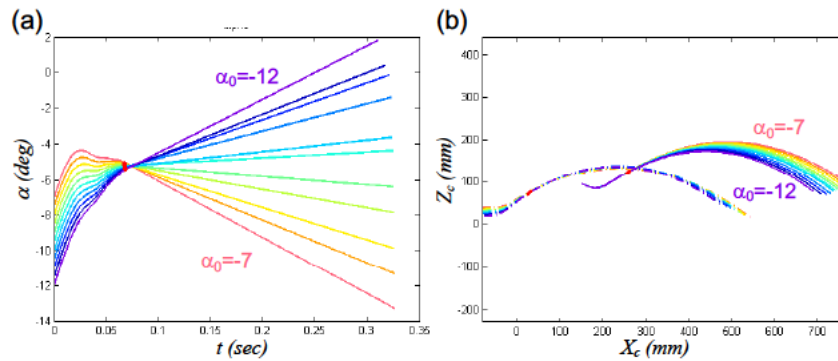


Figure 3. Simulation of various body states versus time with varying initial body pitch α (unit: deg) in the 2nd-step leaping: (a) body pitch and (b) COM trajectory. Red dots represent take-off moment.

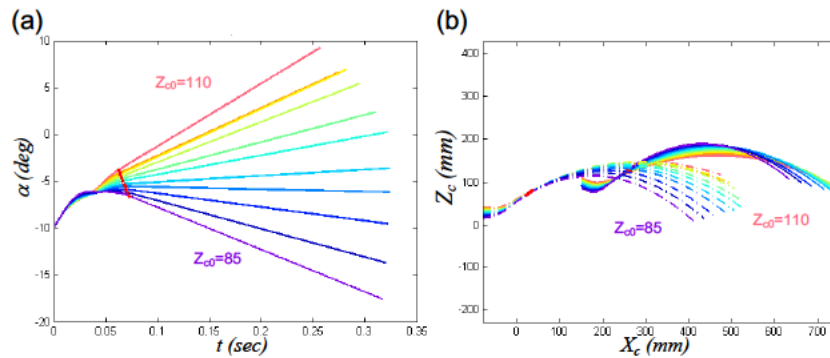


Figure 4. Simulation of various body states versus time with varying initial body heights Z_{c0} (unit: mm) in 2nd-step leaping: (a) body pitch and (b) COM trajectory. Red dots represent take-off moment.

Similar to the model in 1st-step leaping, the initial vertical height Z_{c0} is also the active parameter which can be varied in the 2nd-step leaping. With the body pitch set to -10° , Figure 4 shows variations of various states with time when the robot starts to thrust with full power at different initial robot heights. Figure 4(a) reveals that the initial height also has a significant effect on the overall body pitch trajectory. When the initial body height is higher (i.e., $Z_{c0} = 110$), the body pitch is larger (i.e., head-down), which is undesirable since the robot may hit the ground. In contrast, if initial body height is lower (i.e., $Z_{c0} = 85$), the body pitch remains negative, which may result in the robot's tail colliding with the obstacle. In addition, as shown in Figure 4(b), the flying distance of the robot's tail in this setting is too short. Therefore, a suitable initial body height should be selected—for example, around 0.095m—to yield horizontal flight.

The overall trajectory planning can now be constructed based on the above analysis. In 1st-step leaping, the legs land on the ground with selected body height and then provide full thrust, where the robot moves according to the trajectory shown in Figure 2(b). During the flight, the legs are synchronized and

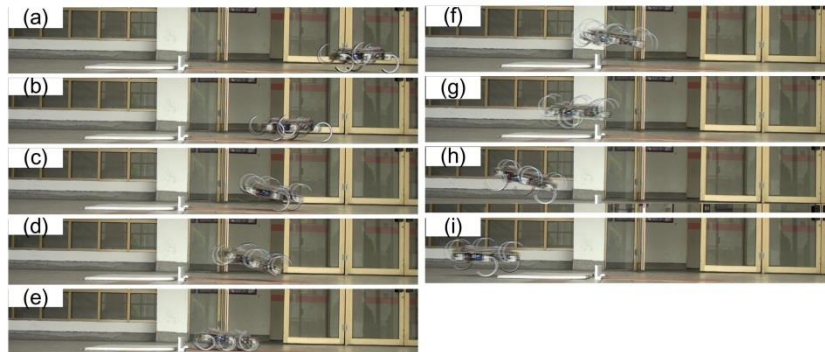


Figure 5. Sequence of images showing the robot leaping over the obstacle.

prepared to land with the desired body height and pitch. After touching the ground, all legs provide full thrust and initiate the 2nd-step leaping, which makes the robot move according to Figure 3(b) or 4(b).

4. Test of the Algorithm on the Empirical Robot

The RHex-style robot is utilized for evaluating leaping behavior. The photo and dimensions of the robot are shown in Figures 1(c) and 1(d). Further detailed specifications robot can be found in [15]. Figure 5 shows sequential images extracted from a video recording of the robot leaping over an obstacle. The height of the obstacle is 95mm. In the beginning, the robot runs toward the obstacle (a). Then the robot starts the leap (b), and takes off for the 1st flight (c). During this flight, two tripods are synchronized (d), preparing for landing with the correct body pitch and height from the ground (e). The robot initiates the 2nd-step leaping and its flight over the obstacle (f) (g). Next, the robot lands on the ground (h) and resumes running (i). Though more detailed investigation is required for evaluation, the video stills mostly confirm that, with the model-based trajectory planning method, the robot can indeed perform leaping behavior.

5. Conclusion

We report on the development of a planar three-legged model for leaping behavior. The model is composed of a rigid body and three massless legs. In order to catch the dynamic characteristics of the half-circle leg of the robot for experimental evaluation, the virtual leg in the R-SLIP model is adopted, which has two segments connected by a torsional spring. With assumption of rolling-contact, the model has 3 DOFs, which can be roughly mapped to the 3 planar states of the robot's COM, including vertical and horizontal motions as well as body pitch. The quantitative equations of motions are formulated and effects of model parameters are investigated. Through variations of the model parameters, a 2-step leaping maneuver is developed. At the 1st step of leaping, the legs land on the ground with specific body height and then provide full thrust. During the flight, the legs in the two tripods are synchronized to align in specific phases,

preparing to land with the desired body height and body pitch. After the robot touches the ground, all legs provide full thrust and initiate the 2nd-step leaping, which makes the body fly over the obstacle. The planned trajectory is also implemented in the RHex-style robot. The video of our initial test shows that the robot can indeed perform leaping behavior.

References

- [1] M. Kovac, M. Fuchs, A. Guignard, J. C. Zufferey, and D. Floreano, "A miniature 7g jumping robot," in *IEEE International Conference on Robotics and Automation*, 2008, pp. 373-378.
- [2] U. Scarfogliero, C. Stefanini, and P. Dario, "The use of compliant joints and elastic energy storage in bio-inspired legged robots," *Mechanism and Machine Theory*, vol. 44, pp. 580-590, Mar 2009.
- [3] R. Niiyama, A. Nagakubo, and Y. Kuniyoshi, "Mowgli: A Bipedal jumping and landing robot with an artificial musculoskeletal system," in *IEEE International Conference on Robotics and Automation*, 2007, pp. 2546-2551.
- [4] B. G. A. Lambrecht, A. D. Horchler, and R. D. Quinn, "A small, insect-inspired robot that runs and jumps," in *IEEE International Conference on Robotics and Automation*, 2005, pp. 1240-1245.
- [5] BostonDynamics. *SandFlea - Leaps small buildings in a single bound*. Available: http://www.bostondynamics.com/robot_sandflea.html
- [6] H. C. Wong and D. E. Orin, "Dynamic control of a quadruped standing jump," in *IEEE International Conference on Robotics and Automation*, 1993, pp. 346-351.
- [7] M. Zucker, N. Ratliff, M. Stolle, J. Chestnutt, J. A. Bagnell, C. G. Atkeson, et al., "Optimization and learning for rough terrain legged locomotion," *International Journal of Robotics Research*, vol. 30, pp. 175-191, Feb 2011.
- [8] D. McMordie and M. Buehler, "Towards pronking with a hexapod robot," in *4th Int. Conf. on Climbing and Walking Robots*, Karlsruhe, Germany, 2001, pp. 659-666.
- [9] J. A. Smith, I. Sharf, and M. Trentini, "Bounding gait in a hybrid wheeled-leg robot," in *IEEE/RSJ International Conference on Intelligent Robots and Systems*, 2006, pp. 5750-5755.
- [10] BostonDynamics. *BigDog - The most advanced rough-terrain robot on Earth* Available: http://www.bostondynamics.com/robot_bigdog.html
- [11] U. Saranli, M. Buehler, and D. E. Koditschek, "RHex: A simple and highly mobile hexapod robot," *International Journal of Robotics Research*, vol. 20, pp. 616-631, Jul 2001.
- [12] K. J. Huang and P. C. Lin, "Rolling SLIP: A model for running locomotion with rolling contact," in *IEEE/ASME International Conference on Advanced Intelligent Mechatronics*, 2012, pp. 21-26.
- [13] E. Z. Moore, D. Campbell, F. Grimmering, and M. Buehler, "Reliable Stair Climbing in the Simple Hexapod 'RHex'," in *IEEE International Conference on Robotics and Automation (ICRA)*, 2002, pp. 2222-2227.
- [14] D. Campbell and M. Buehler, "Stair descent in the simple hexapod 'RHex'," in *IEEE International Conference on Robotics and Automation (ICRA)*, 2003, pp. 1380-1385 vol.1.
- [15] Y. C. Chou, W. S. Yu, K. J. Huang, and P. C. Lin, "Bio-inspired step-climbing in a hexapod robot," *Bioinspiration & Biomimetics*, vol. 7, p. 036008, Sep 2012.